JOURNAL OF AGRICULTURAL AND FOOD CHEMISTRY
ARTICLE

J. Agric. Food Chem. 2009, 57, 10651–10657 10651
DOI:10.1021/jf9028514

Identification of Compounds in Adlay (*Coix lachryma-jobi* L. var. *ma-yuen* Stapf) Seed Hull Extracts That Inhibit Lipopolysaccharide-Induced Inflammation in RAW 264.7 Macrophages

Din-Wen Huang,[†] Cheng-Pei Chung,[†] Yueh-Hsiung Kuo,*[,‡,§,∥] Yun-Lian Lin,*[,⊥] and Wenchang Chiang*[,†]

[†]Graduate Institute of Food Science and Technology, Center for Food and Biomolecules, College of Bioresources and Agriculture, National Taiwan University, Taipei 106, Taiwan, [‡]Tsuzuki Institute for Traditional Medicine, College of Pharmacy, China Medical University, Taichung 404, Taiwan, [§]Agricultural Biotechnology Research, Academia Sinica, Taipei 115, Taiwan, [∥]Department of Chemistry, National Taiwan University, Taipei 106, Taiwan, and [⊥]National Research Institute of Chinese Medicine, Taipei 112, Taiwan, Republic of China

We investigated the effects of adlay seed hull (AH) extracts on the lipopolysaccharide-induced inflammatory response in RAW 264.7 macrophages. An AH ethanol extract (AHE) was partitioned into ethyl acetate, *n*-butanol, and water fractions. Silica gel chromatography of the ethyl acetate fraction yielded 15 subfractions: AHE-Ea-A to AHE-Ea-O. Subfractions AHE-Ea-J, AHE-Ea-K, and AHE-Ea-M had anti-inflammatory activities, as they counteracted the increased cellular production of nitric oxide and prostaglandin E2 induced by lipopolysaccharide by down-regulating inducible nitric oxide synthase and cyclooxygenase 2 expression. Eriodictyol (**1**), the ceramide (2*S*,3*S*,4*R*)-2-[(2′*R*)-2′-hydroxytetracosanoyl-amino]-1,3,4-octadecanetriol (**2**), and *p*-coumaric acid (**3**) were found in the subfractions, and the first two compounds appeared to be primarily responsible for the anti-inflammatory activity. This is the first time that eriodictyol (**1**) and this ceramide (**2**) have been found in AH, and the anti-inflammatory properties of the AHE-Ea fraction can be attributed, at least in part, to the presence of these two compounds.

KEYWORDS: Adlay; anti-inflammatory; nitric oxide; inducible nitric oxide synthase; cyclooxygenase 2; eriodictyol; ceramide

INTRODUCTION

Chronic inflammation causes the up-regulation of several proinflammatory proteins in the effected tissues. Among the numerous proinflammatory enzymes, inducible nitric oxide synthase (iNOS) and cyclooxygenase 2 (COX-2) are the ones that produce nitric oxide (NO) and prostaglandin E2 (PGE_2) in lipopolysaccharide (LPS)-activated macrophages and in other stimulated cells (*1*). At the appropriate physiological levels, NO contributes to vasodilator and neurotransmitter processes, and as part of the immune system, it acts as a defense mechanism against certain pathogens. However, when overproduced in response to LPS stimulation, excess NO can react with superoxide anion radicals to form peroxynitrite, which is a stronger oxidant than NO and can cause a high oxidative stress state (*2*). The resulting inflammation has been shown to be associated with a number of chronic diseases, including asthma, rheumatoid arthritis, inflammatory bowel disease, atherosclerosis, and Alzheimer's disease, and also has a role in various human cancers (*3*).

*To whom correspondence should be addressed. (Y.-H.K.) Tel: 886-2-33661671. E-mail: yhkuo@ntu.edu.tw. (Y.-L.L.) Tel: 886-2-28201999-6531. E-mail: yllin@nricm.edu.tw. (W.C.) Tel: 886-2-33664115. E-mail: chiang@ntu.edu.tw.

Adlay (*Coix lachryma-jobi* L. var. *ma-yuen* Stapf), or Job's tears, is an annual crop that has served as a diuretic and as an anti-inflammatory, antitumor, and analgesic agent in traditional Chinese medicine (*4*). Air-dried adlay seeds can be separated into four parts: the adlay seed hull (AH), adlay testa, adlay bran, and polished adlay. The AH and adlay testa are waste products of adlay seed refinement, with polished adlay and dehulled adlay (polished adlay containing bran) being the edible seeds. We previously found that AH has two distinct physiological activities, an antioxidative activity and an activity that modulates the endocrine system. Kuo and colleagues (*5*) found that the butanol subfraction of the methanol (MeOH) extract of AH had a strong antioxidative activity. Six compounds with antioxidative activities were subsequently identified, including three phenolic compounds (coniferyl alcohol, syringic acid, and ferulic acid) and three lignan compounds (syringaresinol, 4-ketopinoresinol, and mayuenolide). The MeOH extract of AH was found to decrease the release of progesterone and estradiol via a number of different pathways, to inhibit uterine contractions by blocking external Ca^{2+} influx, and to down-regulate testosterone release (*6*−*9*).

Although the antioxidative activities and endocrine-modulating effects of AH have been elucidated, the AH components that have anti-inflammatory activities have yet to be identified. Thus,

Published on Web 11/03/2009

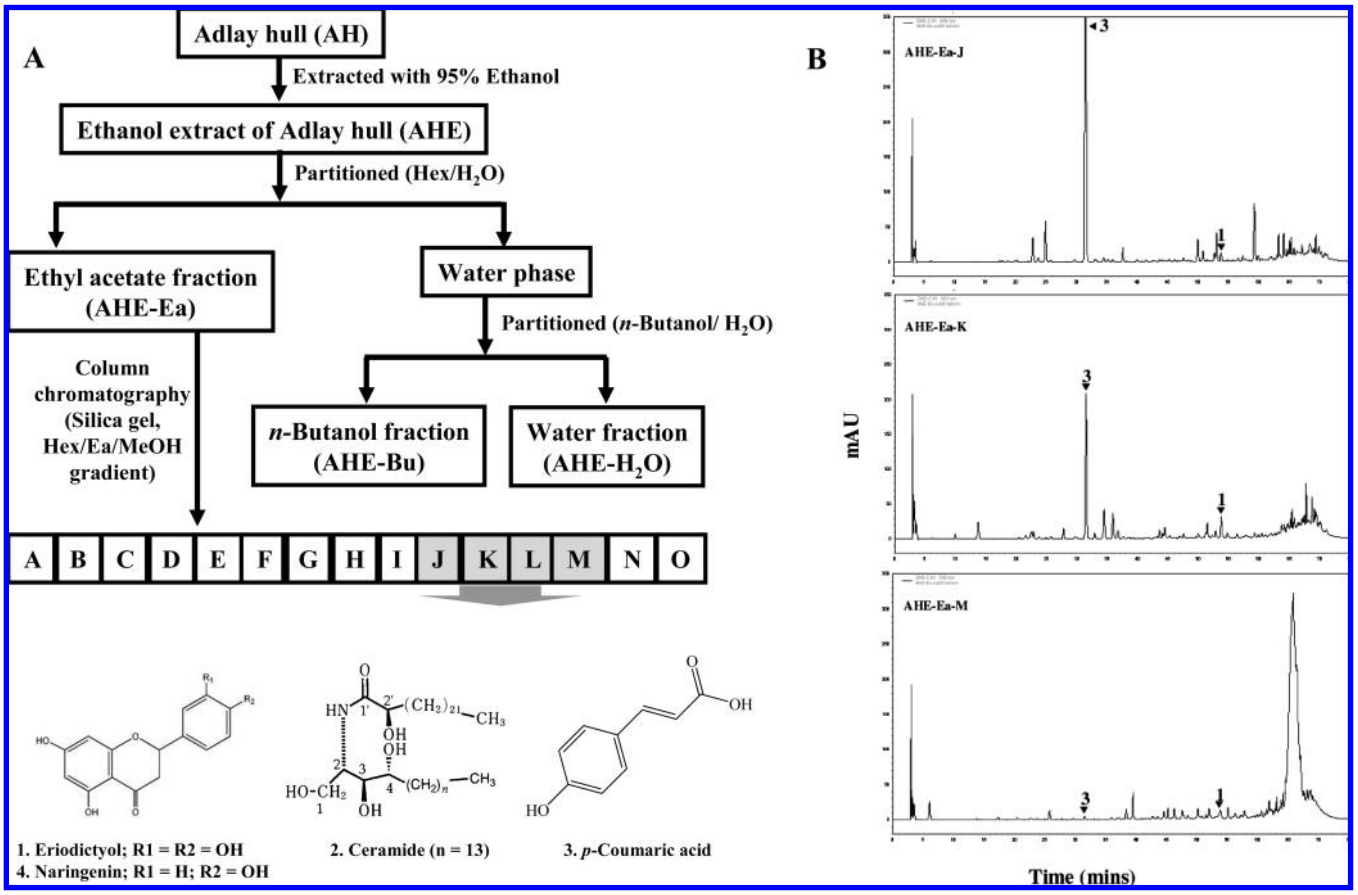

Figure 1. (**A**) Top: A flowchart of the separation methods used to isolate the anti-inflammatory agents of AHs. The AHE-Ea fraction, and its AHE-Ea-J, -K, and -M subfractions, exhibited the most potent anti-inflammatory activities. Bottom: The structures of eriodictyol (**1**), the ceramide (**2**), *p*-coumaric acid (**3**), and naringenin (**4**). (**B**) HPLC chromatograms of the AHE-Ea-J, -K, and -M subfractions. Peaks containing eriodictyol and *p*-coumaric acid are labeled **1** and **3**, respectively.

we sought to determine the mechanisms by which AH inhibits the LPS-induced inflammatory response and the AH components that are responsible for the anti-inflammatory effects.

MATERIALS AND METHODS

Materials. Naringenin, *p*-coumaric acid, chromatographic- and analytical-grade solvents used during the purification procedures and high-performance liquid chromatography (HPLC) [i.e., MeOH, ethanol, hexane, ethyl acetate (EA), butanol, and acetonitrile], and LPS were obtained from Sigma Chemical (St. Louis, MO). Anti-iNOS and anti-COX-2 antibodies were purchased from Upstate (Lake Placid, NY) and BD Biosciences (San Jose, CA), respectively. Anti-β-actin was obtained from Santa Cruz Biotechnology (Santa Cruz, CA). The compatible horseradish peroxidase-conjugated secondary antibodies, goat antirabbit immunoglobulin G, and goat antimouse antibodies were purchased from Pierce (Rockford, IL) and CHEMICON International (Temecula, CA), respectively.

Preparation and Fractionation of the Ethanol AH Extract. AH was processed as described by Hsia et al. (*10*). AH (20 kg) was extracted with three volumes (200 L) of 95% ethanol at room temperature. After each 24 h extraction, the ethanol and AH were separated by filtration. The pooled ethanol filtrates were vacuum evaporated, and the 365 g residue (the AH ethanol extract or AHE; 1.83% of the initial dry weight) was stored at −20 °C. The AHE residue was then suspended in water and partitioned repeatedly with EA until the EA extract was not colored. EA was removed under vacuum, and a 195 g residue (AHE-Ea, 0.98% of the initial dry weight) remained. The residue was dissolved in water and partitioned into butanol. Butanol was removed under vacuum, leaving behind a 45 g residue (AHE-Bu, 0.23% of the initial dry weight). The water fraction was lyophilized, and a 111 g residue (AHE-H_2O, 0.56% of the initial dry weight) was recovered. The anti-inflammatory activities of the various fractions were assessed using the LPS/NO/RAW 264.7 system described below, and only the AHE-Ea fraction had anti-inflammatory activity. The AHE-Ea fraction was subfractionated using silica gel chromatography and a hexane/EA/MeOH gradient. The absorbance of the effluent was monitored at 280 and 340 nm, and 15 subfractions were manually collected and concentrated under vacuum at 60 °C (subfraction A: 0−10% EA/hexane, 0.57 g; subfraction B: ∼10% EA/hexane, 79.77 g; subfraction C: ∼10% EA/hexane, 9.15 g; subfraction D: ∼10% EA/hexane, 1.43 g; subfraction E: ∼10−20% EA/hexane, 2.33 g; subfraction F: ∼20−30% EA/hexane, 1.73 g; subfraction G: ∼30−40% EA/hexane, 2.25 g; subfraction H: ∼40−50% EA/hexane, 2.31 g; subfraction I: ∼50−60% EA/hexane, 2.88 g; subfraction J: ∼60−70% EA/hexane, 1.83 g; subfraction K: ∼70−80% EA/hexane, 4.10 g; subfraction L: ∼90% EA/hexane, 3.28 g; subfraction M: ∼100% EA/hexane, 3.16 g; subfraction N: ∼50−100% MeOH/EA, 32.50 g; and subfraction O: ∼100% MeOH, 3.16 g). The anti-inflammatory activities of the various subfractions were assessed, and subfractions AHE-Ea-J−M were combined and further purified by silica gel column chromatography with a 5−30% MeOH/CH_2Cl_2 gradient and by Sephadex LH-20 chromatography with MeOH as the mobile phase to yield eriodictyol (**1**), a ceramide (**2**), and *p*-coumaric acid (**3**). The structures of the purified compounds were identified by nuclear magnetic resonance (NMR, Bruker AMX-400) and compared with authentic samples. **Figure 1A** shows the flowchart for the extraction of anti-inflammatory compounds from AH.

HPLC Analysis. HPLC analyses were performed according to Huang and colleagues (*11*) using a Hitachi L-6200 intelligent pump equipped with a photodiode array detector (Hitachi L-7455), an automatic injector, and a C18 (150 mm × 4.6 mm, 5 μM) reverse-phase column. Gradient elution was performed with water−2% acetic acid (v/v, solvent A) and water−0.5% acetic acid/acetonitrile (1:1, v/v, solvent B) at a constant

flow rate of 1 mL/min. The gradient steps were as follows: 0−10 min, 5−10% B; 10−40 min, 10−40% B; 40−55 min, 40−55% B; 55−60 min, 55−80% B; 60−65 min, 80−100% B; 65−70 min, 100−50% B; 70−75 min, 50−30% B; 75−80 min, 30−10% B; and 80−85 min, 10−5% B. The column was re-equilibrated with 5% B.

Cell Culture and Stimulation. RAW 264.7 cells (murine) were obtained from the Bioresource Collection and Research Center (Food Industry Research and Development Institute, Hsinchu, Taiwan) and were cultured under a 5% CO_2 atmosphere at 37 °C in Dulbecco's modified Eagle's medium (DMEM) containing 10% heat-inactivated fetal bovine serum, 1% penicillin−streptomycin, and 1% glutamine. To assay the anti-inflammatory effects of the fractions, cells, in serum-free medium, were grown in 6- or 96-well plates or 10 cm dishes for approximately 18−24 h and then treated with only the carrier vehicle (0.1% DMSO), a test fraction, and/or LPS.

MTT Assay for Cell Viability. RAW 264.7 macrophages were added into 96-well plates at a density of 10^5 cells/well and allowed to grow for approximately 18−24 h. Subsequently, the culture medium was replaced, and various test samples in DMSO were added with or without LPS (1 μg/mL) and incubated for an additional 24 h. The concentration of DMSO after dilution in the culture medium was < 0.1%. A filtered methyl thiazole tetrazolium (MTT) solution in serum-free DMEM was added to each well (0.5 mg MTT/mL), and the cells were incubated at 37 °C for 2 h. Unreacted dye was then removed. The insoluble MTT formazan crystals were allowed to dissolve in DMSO at room temperature for 15 min, and the absorbance (at 570 nm) of each sample was measured. The viability of a test sample was calculated using the following equation: % viability = $(\text{absorbance}_{\text{testsample}})/(\text{absorbance}_{\text{control}}) \times 100$.

NO and PGE_2 Formation. RAW 264.7 macrophages were treated in a manner similar to that described for cell viability. In brief, cells were treated with medium alone, with LPS, or with a test sample for 24 h. Thereafter, each supernatant (100 μL) was mixed with the same volume of Griess reagent [1% sulfanilamide in 5% phosphoric acid and 0.1% *N*-(1-naphthyl) ethylenediamine dihydrochloride in water] and incubated for 15 min in the dark. The total amount of nitrite present was calculated based on the absorbance of a sample at 570 nm. The amount of NO synthesized in response to LPS stimulation was calculated using the following equation: % NO synthesis = $[(\text{absorbance}_{\text{sample-treated}} - \text{absorbance}_{\text{control}})/(\text{absorbance}_{\text{LPS-treated}} - \text{absorbance}_{\text{control}})] \times 100\%$. PGE_2 was determined using a commercial PGE_2 kit (Neogen Corp., Lexington, KY). The concentration of PGE_2 was calculated based on the absorbance of a sample at 650 nm.

Western Blotting. RAW 264.7 macrophages were treated in a manner similar to that described for the NO and cell viability assays. Thereafter, cells were washed twice with ice-cold PBS, lysed in 50 mM Tris-HCl (pH 8.0) containing 1 mM NaF, 150 mM NaCl, 1 mM EGTA, 1 mM phenylmethanesulfonyl fluoride, 1% (w/v) NP-40, and 10 μg/mL leupeptin, and then centrifuged at 10000*g* for 30 min at 4 °C. The amounts of cytosolic proteins, recovered in the supernatant, were measured using the Bradford assay, with bovine serum albumin as the standard. To detect iNOS, COX-2, and β-actin, total cytosolic extracts (500 μg protein/mL) were first separated over 8% sodium dodecyl sulfate (SDS)-polyacrylamide minigels and then transferred to Immobilon polyvinylidene difluoride membranes 11 (Millipore, Bedford, MA) using a transfer buffer composed of 25 mM Tris-HCl (pH 8.9), 192 mM glycine, and 20% MeOH. The membranes were each incubated in PBS containing 5% bovine serum albumin for 1 h at room temperature and then overnight at 4 °C in the presence of an appropriate primary antibody (1:1000 dilution of the stock solution). After hybridization with a primary antibody, the membranes were washed with 0.1% (w/v) Tween 20 in PBS three times, incubated with an horseradish peroxidase-labeled secondary antibody overnight at 4 °C, and then washed with the same buffer three more times. To detect the targeted proteins, enhanced chemiluminescence Western blotting reagents (Amersham Pharmacia Biotech) were used. The expression level of each protein relative to that of β-actin was calculated by ImageJ 1.42q.

Statistical Analysis. The data are presented as the mean ± standard deviation. Differences between specific means were analyzed by one-way analysis of variance using the SPSS system, version 11.0 (SPSS, Chicago, IL). Group means were compared using one-way analysis of variance and Duncan's multiple-range test. For comparison of two groups, the Student's *t* test was used. The difference between two means was considered statistically significant when $p < 0.05$ and highly significant when $p < 0.01$.

RESULTS AND DISCUSSION

Identification and Analysis of the Compounds Responsible for the Anti-Inflammatory Activity of Adlay Hull. HPLC was used to quantify the amounts of two of the three purified compounds in the subfractions AHE-Ea-J, AHE-Ea-K, and AHE-Ea-M (chromatograms are shown in **Figure 1B**). When compared with the retention times of known standards (data not shown), the peaks of the AHE-Ea-J, AHE-Ea-K, and AHE-Ea-M chromatograms corresponded to those of eriodictyol (**1**) (5 mg/g in AHE-Ea-J, 10 mg/g in AHE-Ea-K, and 8 mg/g in AHE-Ea-M) and *p*-coumaric acid (**3**) (129 mg/g in AHE-Ea-J, 36 mg/g in AHE-Ea-K, and 2 mg/g in AHE-Ea-M). The ceramide (**2**) was not analyzed using this system. The structures of these three compounds (**Figure 1A**, bottom) were elucidated using one- and two-dimensional NMR spectroscopy and mass spectrometry; these data are presented below.

Eriodictyol (**1**): EIMS, *m*/*z* 288 $[M]^+$. ^{1}H NMR (400 MHz, CD_3OD): δ 6.90 (1H, s, H-2'), 6.76 (1H, d, J = 8.0 Hz, H-6′), 6.74 (1H, d, J = 8.0 Hz, H-5′), 5.88 (1H, d, J = 2.0 Hz, H-6), 5.86 (1H, d, J = 2.0 Hz, H-8), 5.27 (1H, dd, J = 12.8, 3.2 Hz, H-2), 3.06 (1H, dd, J = 17.2, 12.8 Hz, H-3a,), 2.68 (1H, dd, J = 17.2, 3.2 Hz, H-3e). ^{13}C NMR (400 MHz, CD_3OD): δ 197.8 (s, C-4), 168.4 (s, C-7), 165.4 (s, C-5), 164.8 (s, C-9), 146.9 (s, C-4′), 146.5 (s, C-3′), 131.8 (s, C-1′), 119.3 (d, C-6′), 116.2 (d, C-5′), 114.7 (d, C-2′), 103.3 (s, C-10), 97.0 (d, C-6), 96.2 (d, C-8), 80.5 (d, C-2), 44.1 (t, C-3). The data are matched to the reported literature values (*12*).

(2*S*,3*S*,4*R*)-2-[(2′*R*)-2′-Hydroxytetracosanoyl-amino]-1,3,4-octadecanetriol (**2**): ESIMS, *m*/*z* 683 $[M]^-$. ^{1}H NMR (400 MHz, C_5D_5N): δ 8.58 (1H, d, J = 9.2, NH), 5.11 (1H, m, H-2), 4.62 (1H, dd, J = 7.2, 3.2 Hz, H-2′), 4.51 (1H, dd, J = 10.8, 4.4 Hz, H-1), 4.42 (1H, dd, J = 10.8, 4.4 Hz, H-1), 4.32 (1H, dd, J = 6.0, 4.8, H-3), 4.27 (1H, m, H-4), 2.25 (1H, m, H-5), 2.22 (1H, m, H-3′), 2.03 (1H, m, H-3′), 1.94 (1H, m, H-5), 1.91 (1H, m, H-6), 1.74 (1H, m, H-6), 1.32, 1.27 (both brs, total ca. 60H, methylenes), 0.84 (6H, br t, J = 6.8 Hz, H-18 and H-24′). ^{13}C NMR (400 MHz, C_5D_5N): δ 175.2 (s, C-1′), 76.7 (d, C-3), 73.0 (d, C-4), 72.4 (d, C-2′), 62.0 (t, C-1), 52.9 (d, C-2), 35.7 (t, C-3′), 34.1 (t, C-5), 26.6 (t′, C-6), 14.3 (q, C-18 and C-24′). The data are matched to the reported literature values (*13*).

p-Coumaric acid (**3**) was identified by comparison with an authentic sample and reported data (*14*).

Effects of AHE, Partitioned Fractions, and Subfractions on LPS-Induced NO and PGE_2 Production in RAW 264.7 Cells. Normal cellular concentrations of NO have a positive impact on cell function, whereas excessive NO levels can have detrimental effects. When present at normal nanomolar concentrations, NO acts as a signaling molecule involved in vasodilation and neurotransmission and as a defensive immunological agent in disease states. When produced at higher concentrations in response to LPS, however, NO is an inflammatory agent (*2*). Adlay seeds have been used as an anti-inflammatory agent in traditional Chinese medicine (*4*). The purpose of this report was to identify the compounds in AH that mediate the observed anti-inflammatory effects of adlay seeds. **Figure 2** diagrams the effects of AHE and its fractions (2.5−20 μg/mL) on the formation of NO in RAW 264.7 macrophages stimulated with LPS (1 μg/mL). NO production decreased slightly in the presence of the AHE, AHE-Bu, and AHE-H_2O fractions, whereas NO production was significantly inhibited by the AHE-Ea fraction in a dose-dependent manner. The IC_{50} value for AHE-Ea was 14 μg/mL, which

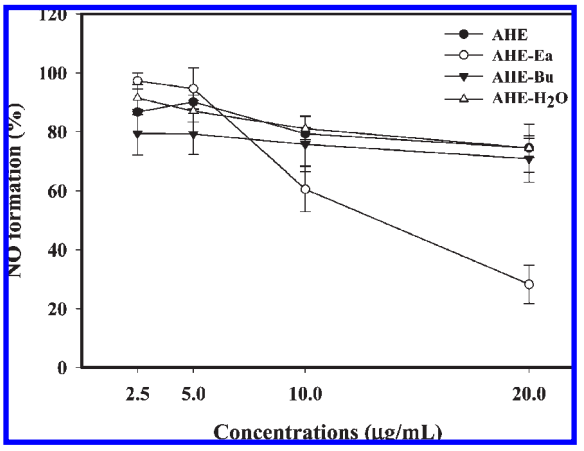

Figure 2. Effects of AHE and its fractions on LPS-induced NO production in RAW 264.7 macrophages. The cells were tested after treatment for 24 h with AHE or fractions AHE-Ea, AHE-Bu, or AHE-H_2O (2.5−20 μg/mL) and LPS (1 μg/mL).

compares favorably with our previously reported value of 5 μg/mL for resveratrol (*11*).

Because AHE-Ea was the most effective inhibitor of NO production, we used silica gel chromatography to separate this fraction into 15 subfractions that were then tested for their anti-inflammatory activity. The inhibitory effects of the AHE-Ea subfractions (5 μg/mL) on LPS-induced NO formation in RAW 264.7 macrophages are shown in **Figure 3A**. The AHE-Ea-J, AHE-Ea-K, and AHE-Ea-M subfractions had the greatest inhibitory activity ($p < 0.05$). Not only did AHE-Ea (10 μg/mL), AHE-Ea-J (5 μg/mL), AHE-Ea-K (5 μg/mL), and AHE-Ea-M (5 μg/mL) inhibit NO formation, but these fractions also inhibited PGE_2 formation in the LPS-induced macrophages (**Figure 3B**). Resveratrol was used as the positive control.

The viability of control RAW 264.7 macrophages and those treated with the test samples and/or LPS for 24 h was assessed by the MTT assay. None of the test samples affected macrophage viability (data not shown), indicating that the inhibitory effects of the test samples were not attributable to cytotoxicity.

Eriodictyol (**1**), the ceramide (**2**), and *p*-coumaric acid (**3**) were identified in the three subfractions AHE-Ea-J, AHE-Ea-K, and AHE-Ea-M. This is the first time that eriodictyol (**1**) and ceramide (**2**) have been found in AH. The amount of *p*-coumaric acid decreased significantly with elution time during the chromatography of the AHE-Ea fraction, whereas the amount of eriodictyol was relatively constant. However, the effects of the AHE-Ea-J and AHE-Ea-M subfractions on lowering NO formation did not differ. Therefore, the anti-inflammatory effects of the AHE-Ea-J, AHE-Ea-K, and AHE-Ea-M subfractions were probably mainly a consequence of the eriodictyol content rather than the *p*-coumaric acid content. This finding agrees with that of our previous study (*11*): The IC_{50} value of *p*-coumaric acid for the inhibition of NO production was greater than that of eriodictyol (437 and 8 μg/mL, respectively). Although *p*-coumaric acid had been shown to have a weak anti-inflammatory effect on NO formation, it may have influenced the anti-inflammatory effects of the subfractions AHE-Ea-J, AHE-Ea-K, and AHE-Ea-M because it was present at high concentrations.

Effects of AHE-Ea, AHE-Ea-J, AHE-Ea-K, and AHE-Ea-M on LPS-Induced iNOS and COX-2 Expression in RAW 264.7 Cells. COX-2 and iNOS are critical and necessary components of the inflammation pathways that produce NO and PGE_2 (*15*). As such, Western blotting was used to determine whether the test samples inhibited LPS-induced expression of COX-2 and iNOS in

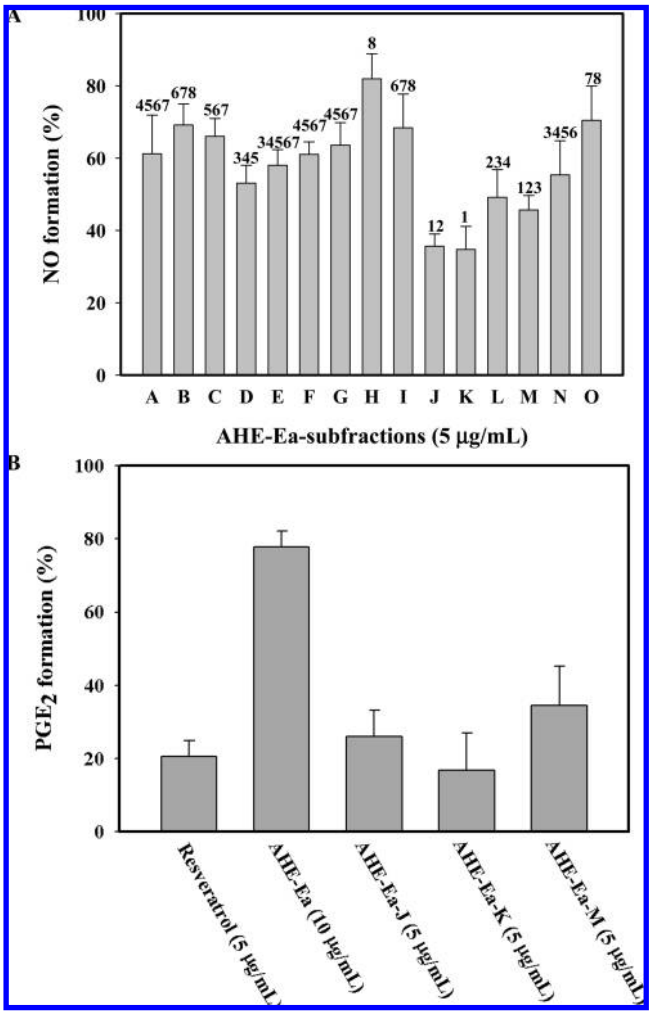

Figure 3. Effects of various AHE-Ea subfractions on LPS-induced NO production (**A**) and PGE2 formation (**B**) in RAW 264.7 macrophages. The cells were tested after treatment for 24 h with different subfractions of AHE-Ea (5 μg/mL) and LPS (1 μg/mL). In panel **A**, columns that do not share a common number are significantly different ($p < 0.05$), and the smaller number means the better inhibitory effects of AHE-Ea subfractions on NO formation.

RAW 264.7 macrophages. The cells that were treated with LPS (1 μg/mL) dramatically increased their expression of COX-2 and iNOS. Treatment with AHE-Ea (10 μg/mL) or with AHE-Ea-J, AHE-Ea-k, or AHE-Ea-M (each 5 μg/mL) inhibited LPS-induced COX-2 and iNOS expression (**Figure 4**).

Effects of Eriodictyol (1), Ceramide (2), and Naringenin (4) on LPS-Induced NO and PGE_2 Formation in RAW 264.7 Cells. Naringenin (**4**), a similar flavanone, was isolated from AH in our previous study (*8*). Thus, the effect of naringenin on NO production was compared with the effects of eriodictyol (**1**) and the ceramide (**2**). RAW 264.7 macrophages were treated with or without eriodictyol (**1**), the ceramide (**2**), and naringenin (**4**) at concentrations between 2.5 and 20 μg/mL in the absence or presence of LPS for 24 h. The effects of eriodictyol (**1**), ceramide (**2**), and naringenin (**4**) on cell viability and PGE_2 and NO formation are shown in **Figure 5**. PGE_2 and NO formation gradually decreased in a dose-dependent manner when the cells were treated with eriodictyol (**1**), the ceramide (**2**), or naringenin (**4**). Eriodictyol (**1**), however, more potently inhibited NO production as compared with the ceramide (**2**) or naringenin (**4**) (IC_{50} = 8, 19, and 18 μg/mL, respectively; **Figure 5A**).

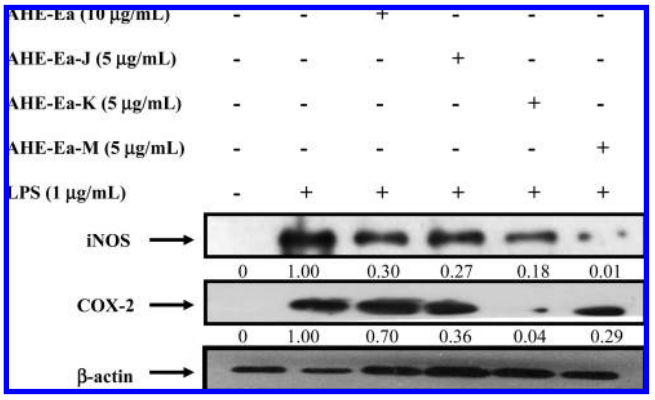

Figure 4. Effects of the AHE-Ea fraction and the AHE-Ea-J, AHE-Ea-K, and AHE-Ea-M subfractions on LPS-induced expression of iNOS and COX-2 in RAW 264.7 macrophages. Cells were first incubated in the absence of LPS (lane 1) or with LPS (1 μg/mL, lanes 2−6), and then, the ATE-Ea fraction (lane 3) or subfraction AHE-Ea-J (lane 4), AHE-Ea-K (lane 5), or AHE-Ea-M (lane 6) was added/incubated with the LPS-treated cells, as indicated. After incubation, equal amounts of total protein (500 μg/mL) were subjected to SDS-PAGE, and the expression of iNOS, COX-2, and β-actin was detected by Western blotting. The numbers below the iNOS and COX-2 lanes indicate the amount of each protein in each sample relative to the amount of β-actin found in each sample.

Treatment with eriodictyol (**1**) or the ceramide (**2**) at concentrations ranging from 2.5 to 20 μg/mL did not kill macrophages. However, at a concentration of 20 μg/mL, naringenin (**4**) was indeed cytotoxic (**Figure 5C**). Thus, concentrations of eriodictyol (**1**), ceramide (**2**), and naringenin (**4**) that did not kill the cells were used for further experimentation.

Effects of Eriodictyol (1), Ceramide (2), and Naringenin (4) on LPS-Induced iNOS and COX-2 Expression in RAW 264.7 Macrophages. The effects of eriodictyol (**1**), ceramide (**2**), and naringenin (**4**) on LPS-induced iNOS and COX-2 expression in RAW 264.7 cells were examined by Western blot analysis. As shown in **Figure 6**, macrophages treated with LPS (1 μg/mL) had significantly increased COX-2 and iNOS expression as compared with the control experiment performed in the absence of LPS. Eriodictyol (**1**) and the ceramide (**2**), at concentrations of about 5−10 and 10−20 μg/mL, respectively, were added to the medium simultaneously with LPS. Both compounds inhibited iNOS expression. However, iNOS expression was only slightly down-regulated in the presence of 5−10 μg/mL naringenin (**4**). The ceramide (**2**) and naringenin (**4**) both inhibited COX-2 expression in a dose-dependent manner. Although COX-2 expression was not down-regulated by eriodictyol (**1**), PGE_2 production was decreased (**Figure 5B**), indicating that eriodictyol (**1**) may directly inhibit COX-2 enzyme activity.

Ceramides are composed of a sphingosine and a fatty acid chain. Ceramide structures vary according to the degree of saturation, fatty acid chain length, and the extent to which the *N*-linked fatty acids are α-hydroxylated. Distinct ceramides may participate in different regulatory pathways and cellular responses to external stimuli (*16*). In this study, we observed not only an inhibitory effect of the ceramide (**2**) on LPS-induced NO formation but also the down-regulation of the expression of the inflammatory-related proteins, iNOS and COX-2 (**Figures 5** and **6**). Hsu and colleagues (*17*) have reported that a cell-permeable ceramide analogue (C_2-ceramide) reduced the formation of NO and PGE_2 in LPS-treated RAW 264.7 macrophages by down-regulating the expression of iNOS and COX-2, in addition to reducing the activation of NF-κB and AP-1. CD14, the high-affinity receptor for LPS in myeloid cells, recognizes LPS in the

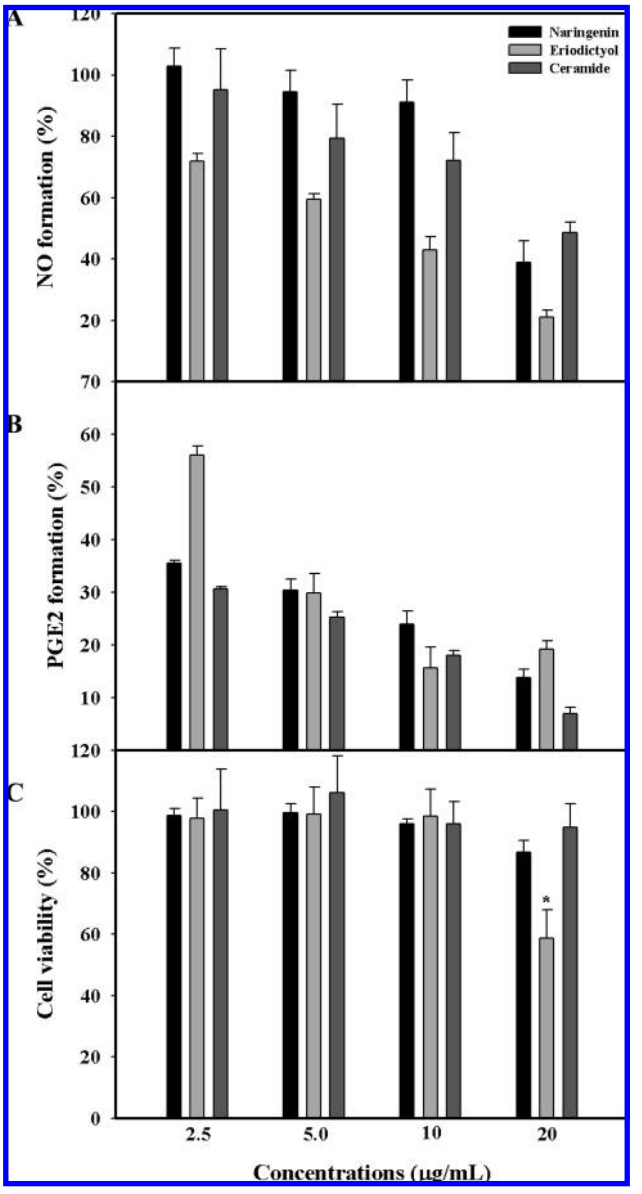

Figure 5. Effects of eriodictyol (**1**), the ceramide (**2**), and naringenin (**4**) on LPS-induced NO formation (**A**), PGE_2 formation (**B**), and cell viability (**C**) in RAW 264.7 macrophages. The cells were tested after treatment for 24 h with naringenin, eriodictyol, or the ceramide (2.5−20 μg/mL) and LPS (1 μg/mL).

LPS-binding protein complex (*18*). The core structure of LPS is lipid A, which has structural similarity with ceramides (*19*, *20*). Thus, LPS may be a structural mimic of ceramides (*21*). Therefore, the inhibitory effects of the ceramide (**2**) on LPS-induced inflammation may be the result of a competition for CD14 between LPS and the ceramide (**2**). Conversely, Haus and colleagues (*22*) found an increased total ceramide concentration in the blood of type 2 diabetics and also found that their insulin sensitivities correlated inversely with the total amount of ceramides present via the induction of inflammatory mediators, such as TNF-α. Ceramides were also found to enhance TNF-α-induced COX-2 activation by first activating NF-κB and the production of reactive oxygen species in mesangial cells (*23*). The anti-inflammatory or pro-inflammatory effect of various kinds of ceramides may be determined by the number of hydroxyl groups that they contain; both C_2-ceramide and AH-ceramide have four additional hydroxyl groups as compared with the other types of ceramides mentioned above.

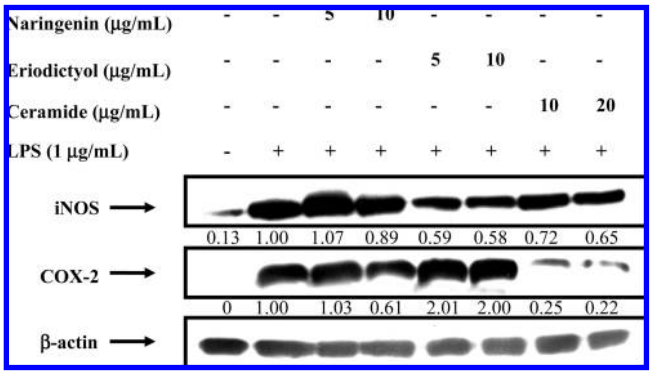

Figure 6. Effects of eriodictyol (**1**), the ceramide (**2**), and naringenin (**4**) on LPS-induced iNOS and COX-2 expression in RAW 264.7 macrophages. Cells were incubated in the absence of LPS (lane 1) or with LPS (1 μg/mL, lanes 2−8), and then, eriodictyol (**1**), the ceramide (**2**), or naringenin (**4**) at 5, 10, or 20 μg/mL was added/incubated with the LPS-treated cells, as indicated. At the end of incubation, equal amounts of total protein (500 μg/mL) were subjected to SDS-PAGE, and the expression of iNOS, COX-2, and β-actin was detected by Western blotting. The numbers below the iNOS and COX-2 lanes indicate the amount of each protein in each sample relative to the amount of β-actin found in each sample.

Our previous study showed that AH contains naringenin (*8*). However, in the present study, naringenin was not found in the AHE-Ea-J, AHE-Ea-K, and AHE-Ea-M subfractions, possibly because the naringenin concentrations in the AHE-Ea-J, AHE-Ea-K, and AHE-Ea-M subfractions were below the HPLC detection limit. Both naringenin and eriodictyol are flavanones. Therefore, the anti-inflammatory effects of both compounds were investigated in this study. Eriodictyol more effectively down-regulated NO formation (**Figure 5**), and this result agrees with the relative suppression levels of iNOS expression by these two flavanones (**Figure 6**). Eriodictyol has two hydroxyl groups at the 3′- and 4′-positions of the B ring, whereas naringenin has only one hydroxyl group at the 4′-position of the B ring. It is increasingly appreciated that flavonoids with hydroxyls at the B ring 3′- and 4′-positions are those that have anti-inflammatory activities (*24*, *25*).

The IC_{50} value of the AHE-Ea fraction for inhibition of LPS-induced NO formation in RAW 264.7 macrophages was 14 μg/mL, slightly lower than that found for the ceramide (**2**) and higher than that found for the eriodictyol (**1**). Therefore, phytochemicals of the AHE-Ea fraction may act synergistically to inhibit the LPS-induced inflammatory response. Similarly, RE568, the ethanol extract of red mold rice, also has been shown to more strongly repress amyloid β-peptide-induced cell damage than equivalent amounts of its fractionated components (*26*).

In conclusion, it appears that eriodictyol (**1**) and the ceramide (**2**) isolated from AH are at least partially responsible for the observed anti-inflammatory effects of the AHE-Ea fraction. They do so by inhibiting NO formation and down-regulating iNOS and COX-2 expression. Thus, the AHE-Ea fraction and/or components thereof may be efficacious for treatment of inflammatory-mediated disease, and *p*-coumaric acid, because of its high level in the AHE-Ea fraction, may potentiate the therapeutic targeting of other components in this fraction.

LITERATURE CITED

(1) Shin, K. M.; Kim, I. T.; Park, Y. M.; Ha, J.; Choi, J. W.; Park, H. J.; Lee, T. S.; Lee, K. T. Anti-inflammatory effect of caffeic acid methyl ester and its mode of action through the inhibition of prostaglandin E2, nitric oxide and tumor necrosis factor-a production. *Biochem. Pharmacol.* **2004**, *68*, 2327–2336.

(2) Fang, S. C.; Hsu, C. L.; Yen, G. C. Anti-inflammatory effects of phenolic compounds isolated from the fruits of *Artocarpus heterophyllus*. *J. Agric. Food Chem.* **2008**, *56*, 4463–4468.

(3) Yamamoto, Y.; Gaynor, R. B. Therapeutic potential of the NF-κB pathway in the treatment of inflammation and cancer. *J. Clin. Invest.* **2001**, *107*, 135–142.

(4) Hsia, S. M.; Chiang, W.; Kuo, Y. H.; Wang, P. S. Downregulation of progesterone biosynthesis in rat granulosa cells by adlay (*Coix lachryma-jobi* L. var. *ma-yuen* Stapf) bran extracts. *Int. J. Impotence Res.* **2006**, *18*, 264–274.

(5) Kuo, C. C.; Chiang, W.; Liu, G. P.; Chien, Y. L.; Chang, J. Y.; Lee, C. K.; Lo, J. M.; Huang, S. L.; Shih, M. C.; Kuo, Y. C. 2,2′-Diphenyl-1-picrylhydrazyl radical-scavenging active components from adlay (*Coix lachryma-jobi* L. var. *ma-yuen* Stapf) hulls. *J. Agric. Food Chem.* **2002**, *50*, 5850–5855.

(6) Chang, L. L.; Wun, A. W.; Hung, C. T.; Hsia, S. M.; Chiang, W.; Wang, P. S. Effects of crude adlay hull acetone extract on corticosterone release from rat zona fasciculata-reticularis cells. *Naunyn-Schmiedeberg's Arch. Pharmacol.* **2006**, *374*, 141–152.

(7) Hsia, S. M.; Yeh, C. L.; Kuo, Y. H.; Wang, P. S.; Chiang, W. Effects of adlay (*Coix lachryma-jobi* L. var. *ma-yuen* Stapf) hull extracts on the secretion of progesterone and estradiol *in vivo* and *in vitro*. *Exp. Biol. Med.* **2007**, *232*, 1181–1194.

(8) Hsia, S. M.; Kuo, Y. H.; Chiang, W.; Wang, P. S. Effects of adlay hull extracts on uterine contraction and Ca^{2+} mobilization in the rat. *Am. J. Physiol. Endocrinol. Metab.* **2008**, *295*, E719–E726.

(9) Hsia, S. M.; Tseng, Y. W.; Wang, S. W.; Kuo, Y. H.; Huang, D. W.; Wang, P. S.; Chiang, W. Effect of adlay (*Coix lachryma-jobi* L. var. *ma-yuen* Stapf) hull extracts on testosterone release from rat Leydig cells. *Phytother. Res.* **2009**, *23*, 687–695.

(10) Hsia, S. M.; Chiang, W.; Kuo, Y. H.; Wang, P. S. Downregulation of progesterone biosynthesis in rat granulosa cells by adlay (*Coix lachryma-jobi* L. var. *ma-yuen* Stapf) bran extracts. *Int. J. Impotence Res.* **2006**, *18*, 264–274.

(11) Huang, D. W.; Kuo, Y. H.; Lin, F. Y.; Lin, Y. L.; Chiang, W. Effect of adlay (*Coix lachryma-jobi* L. var. *ma-yuen* Stapf) testa and its phenolic components on Cu^{2+}-treated low-density lipoprotein (LDL) oxidation and lipopolysaccharide (LPS)-induced inflammation in RAW 264.7 macrophages. *J. Agric. Food Chem.* **2009**, *57*, 2259–2266.

(12) Zhang, X.; Hung, T. M.; Phuong, P. T.; Ngoc, T. M.; Min, B. S.; Song, K. S.; Seong, Y. H.; Bae, K. Anti-inflammatory activity of flavonoids from *Populus davidiana*. *Arch. Pharm. Res.* **2006**, *29*, 1102–1108.

(13) Huang, Q.; Tezuka, Y.; Hatanaka, Y.; Kikuchi, T.; Nishi, A.; Tubaki, K. Studies on metabolites of mycoparasitic fungi. III.[1] new sesquiterpene alcohol from *Trichoderma koningii*. *Chem. Pharm. Bull.* **1995**, *43*, 1035–1038.

(14) Takahashi, H.; Iuchi, M.; Fujita, Y.; Minami, H.; Fukuyama, Y. Coumaroyl triterpenes from *Casuarina equisetifolia*. *Phytochemistry* **1999**, *51*, 543–550.

(15) Shin, S. D.; Fabris, M.; Ferrari, V.; Carbonare, M. D.; Leon, A. Quercetin protects cutaneous tissue-associated cell types including sensory neurons from oxidative stress induced by glutathione depletion: Cooperative effects of ascorbic acid. *Free Radical Biol. Med.* **2004**, *22*, 669–678.

(16) Alwani, M. E.; Wu, B. X.; Obeid, L. M.; Hannun, Y. A. Bioactive sphingolipids in the modulation of the inflammatory response. *Pharmacol. Ther.* **2006**, *112*, 171–183.

(17) Hsu, Y. W.; Chi, K. H.; Huang, W. C.; Lin, W. W. Ceramide inhibits lipopolysaccharide-mediated nitric oxide synthase and cyclooxygenase-2 induction in macrophages: Effects on protein kinases and transcription factors. *J. Immunol.* **2001**, *166*, 5388–5397.

(18) Sweet, M. J.; Hume, D. A. Endotoxin signal transduction in macrophages. *J. Leukocyte Biol.* **1996**, *60*, 8–26.

(19) Morrison, D. K.; Kaplan, D. R.; Rapp, U.; Robberts, R. M. Signal transduction from membrane to cytoplasm: Growth factors and membrane-bound oncogene products increase Raf-1 phosphorylation and associated protein kinase activity. *Proc. Natl. Acad. Sci. U.S.A.* **1988**, *85*, 8855–8859.

(20) Joseph, C. K.; Wright, S. D.; Bornmann, W. G.; Randoph, J. T.; Kumar, E. R.; Bittman, R.; Liu, J.; Klesnick, R. N. Bacterial lipopolysaccharide has structural similarity to ceramide and stimulates ceramide-activated protein kinase in myeloid cells. *J. Biol. Chem.* **1994**, *269*, 17606–17610.

(21) Wright, S. D.; Kolesnick, R. N. Does endotoxin stimulate cells by mimicking ceramide? *Immunol. Today* **1995**, *16*, 297–302.

(22) Haus, J. M.; Kashyap, S. R.; Kasumov, T.; Zhang, R.; Kelly, K. R.; Defronzo, R. A.; Kirwan, J. P. Plasma ceramides are elevated in obese subjects with type 2 diabetes and correlate with the severity of insulin resistance. *Diabetes* **2009**, *58*, 337–343.

(23) Kitatani, K.; Akiba, S.; Sato, T. Ceramide-induced enhancement of secretory phospholipase A_2 expression via generation of reactive oxygen species in tumor necrosis factor-a-stimulated mesangial cells. *Cell. Signalling* **2004**, *16*, 967–974.

(24) Comalada, M.; Ballester, I.; Bailón, E.; Sierra, S.; Xaus, J.; Glávez, J.; de Medina, F. S.; Zarzuelo, A. Inhibition of pro-inflammatory markers in primary bone marrow-derived mouse macrophages by naturally occurring flavonoids: Analysis of the structure-activity relationship. *Biochem. Pharmacol.* **2006**, *72*, 1010–1021.

(25) Lee, J. K.; Kim, S. Y.; Kim, Y. S.; Lee, W. H.; Hwang, D. H.; Lee, J. Y. Suppression of the TRIF-dependent signaling pathway of toll-like receptors by luteolin. *Biochem. Pharmacol.* **2009**, *77*, 1391–1400.

(26) Lee, C. L.; Wang, J. J.; Pan, T. M. Red mold rice extract represses amyloid beta peptide-induced neurotoxicity via potent synergism of anti-inflammatory and antioxidative effect. *Appl. Microbiol. Biotechnol.* **2008**, *79*, 829–841.

Received for review August 14, 2009. Revised manuscript received October 14, 2009. Accepted October 15, 2009.